Evidence of Shear-Induced Fluid Fracture in Telechelic Polymer Networks

J.-F. Berret
Complex Fluids Laboratory, CNRS–Cranbury Research Center Rhodia Inc., 259 Prospect Plains Road CN 7500, Cranbury, New Jersey 08512

Y. Séréro
FOM–Institute for Atomic and Molecular Physics, Kruislaan 407, 1098 SJ, Amsterdam, The Netherlands
(Received 22 January 2001; published 10 July 2001)

The shear-flow properties of telechelic polymer networks have been investigated by rheology and flow-visualization techniques. The steady-shear viscosity versus shear-rate curves exhibits two main branches separated by a discontinuity. One branch of the flow curve is Newtonian and shear thickening, whereas the second one is shear thinning. Above the discontinuity, shear induces a fluid fracture similar to those reported for brittle solids and at the origin of an inhomogeneous flow. Because of the finite relaxation time of the polymer network however, and contrary to ordinary gels, the fracture can be created and healed reversibly.

DOI: 10.1103/PhysRevLett.87.048303 PACS numbers: 83.80.–k

When submitted to steady deformation rates, many complex fluids such as surfactant and block copolymer solutions, microemulsions, and colloidal dispersions exhibit a rheological transition. In planar shear flow, rheological transitions manifest themselves by some anomaly in the shear-stress versus shear-rate behavior and from their phenomenology, these anomalies bear strong similarities with equilibrium phase transitions [1]. Despite intense theoretical and experimental efforts undertaken these last years, these transitions are still not understood. It has been suggested recently that associating polymers in solutions also display a transition induced by shear [2–5]. Since the microstructure and linear rheology of these self-assembled fluids are by now well established [3,6,7], it is our hope to identify the features of the transition more easily and to shed some light on its thermodynamic or mechanical nature.

Associating polymers are water-soluble polymers that are modified chemically by the adjunct of hydrophobic substituents on or along the backbone [7]. One of the simplest associating polymers is the telechelic for which the substitution takes place at the two extremities of the chains. At low concentrations, telechelic polymers self-assemble in water into monodisperse flowerlike micelles. From their local structure, these flowerlike micelles compare well with star polymers or with diblock copolymer micelles. Aggregation numbers are composed between 20–50, depending on the length of the hydrophobes. In some cases, a phase separation occurs [3,6]. Above a second threshold noted c^*, around 1% in weight percent, the fluid undergoes a transition with the formation of an infinite and multiconnected network. The flowerlike micelles are the nodes of this network, and the elastically active links are polymeric chains with both end caps attached to neighboring micelles. In this network regime, three subregimes can be distinguished. (i) Slightly above c^*, the microstructure and rheology of the fluid are determined by percolation theories [8]. (ii) For $c > c^*$, the network connectivity is high, and the viscoelasticity is controlled by the mechanism of disengagement of the end caps from the hydrophobic cores, yielding a single exponential stress relaxation function. (iii) For $c \gg c^*$, the deformation of the micellar corona under close packing takes place and enhances the network elasticity [3,6]. Eventually, at still higher concentration, cubic mesophases may appear [9].

In this Letter, we investigate the nonlinear rheological responses for viscoelastic solutions in the intermediate regime of concentration, $c > c^*$. The physico-chemical experimental conditions such as concentration, temperature, and molecular weights were adjusted so as to build a reversible cross-linked network of high connectivity and where the active links connect only the nearest neighbor micelles. The main result here is the observation of a shear-induced fluid fracture similar to those found in brittle solids and at the origin of an inhomogeneous shear flow in the shear-thinning regime.

We have recently started a systematic study of the rheology and of the microstructure of telechelics aqueous solutions [10]. Polymers with a poly(ethylene oxide) (PEO) middle block and semiperfluorinated end caps were synthesized. We have explored a broad range of chemical architectures, changing either the length of the soluble chains or the nature of the spacer linking the end caps to the ethylene oxide chains. As a result, we have found that in the intermediate regime of concentration ($c > c^*$), the telechelics solutions are viscoelastic and close to Maxwellian fluids. Interestingly, the Maxwell relaxation time τ was found to depend noticeably on the fine structure of the triblock architecture, ranging from 0.01 to 100 s. For the present work we have selected two telechelic systems characterized by different relaxation times. The first polymer has a PEO middle block (molecular weight 10 000 g/mol), and the link to the semifluorinated end caps $C_8F_{17}(CH_2)_{11}$ is ensured by an isophorone diurethane group. The second

telechelic uses the same end caps, but the soluble chain is twice as long and the spacer is an ester function. By analogy with hydrophobically ethoxylated urethane (HEUR) telechelics [7], the first polymer is termed F-HEUR, whereas the telechelic with the ester spacer is abbreviated as FA-PEO. Details on the synthesis and characterization of these polymers can be found elsewhere [5,10]. The mechanical properties were investigated using a strain-controlled rheometer (Rheometrics® Fluid Spectrometer) equipped with a cone-and-plate configuration (angle 0.02 rad, radii 30 or 50 mm).

Figure 1 displays results of linear and nonlinear rheology performed on aqueous solutions made from FA-PEO (open symbols) and F-HEUR (closed symbols), both at the concentration $c = 4\%$. In the inset, the linear response of the two fluids is illustrated by the time dependence of their stress relaxation functions $G(t)$. The time decay is described in terms of a stretched exponential of the form $G(t) = G_0 \exp[-(t/\tau)^{\alpha}]$, where G_0 denotes the elastic modulus extrapolated as $t \to 0$, τ is the viscoelastic relaxation time, and α the stretched exponent. For FA-PEO, one gets $\tau = 0.6$ s (at $T = 25\,^{\circ}\mathrm{C}$) and $\alpha = 0.82$, and for the F-HEUR system, $\tau = 6$ s (at $T = 35\,^{\circ}\mathrm{C}$) and $\alpha = 0.81$. The steady shear viscosity behavior is shown in Fig. 1 as a function of the applied shear rate in reduced units. The viscosity η has been normalized by its zero-shear value η_0 whereas $\dot{\gamma}$ is expressed in units of $1/\tau$. For the two telechelic solutions, the flow curves $\eta/\eta_0(\Gamma)$ where $\Gamma = \dot{\gamma}\tau$ are very similar and show three regimes. At low shear rates, the fluid exhibits a Newtonian behavior, $\eta/\eta_0 = 1$. Shear thickening is then observed above $\Gamma_1 \sim 0.1$, followed by a strong decrease of the viscosity (shear thinning). The shear-thinning behavior is associated with a discontinuity, corresponding to a vertical drop in $\eta/\eta_0(\Gamma)$ at $\Gamma_2 \sim 0.6$. The discontinuity in the flow curves of Fig. 1 has been evidenced using time-resolved measurements in start-up experiments. In Fig. 2, we show transient viscosity data obtained for the FA-PEO solution (same sample as in Fig. 1) at shear rates close to Γ_2. For shear rates below 0.546, $\eta(t)$ quickly rises up and reaches its stationary value within a time of the order of several τ's. At a slightly higher rate, $\Gamma = 0.552$, the viscosity behaves similarly during an induction period of ~500 s, and then slowly decreases at a level which is below that of the previous shear rate by 40%. This decrease becomes more and more rapid as Γ is further increased. The divergence of the equilibrium time of the stress as $\Gamma - \Gamma_2 \to 0^+$ is the signature of a discontinuity in the flow curve. The typical time to reach steady state in Fig. 2 was actually found to vary as $(\Gamma - \Gamma_2)^{-1}$ [5]. This result will not be discussed here, but it means that at high shear rates, this time becomes again of the order of the relaxation time τ of the fluid. In the present case, since τ is close to the response time of the rheometer (~100 ms), this prevents us from observing the transient kinetics for the stress in the high shear-rate region. In order to circumvent this drawback, we utilize the property shown in Fig. 1, namely, the universality of the nonlinear rheological behaviors in the intermediate regime of concentrations.

We have performed start-up measurements on a F-HEUR solution at a concentration of 4% and the results are shown in Fig. 3 for rates Γ composed between 3 and 18. The linear viscoelastic parameters for this solution are $G_0 = 53$ Pa and $\tau = 57$ s. The increase of the network relaxation time with respect to that of Fig. 1 was obtained by taking advantage of its Arrhenius temperature dependence (with an energy barrier of $45 k_B T$ or 102 kJ/mole [5]) and by reducing the temperature to 20 °C. The stress kinetics in Fig. 3 can be decomposed as follows. At low deformation, $\gamma < 0.5$, the stress increases linearly. Above 0.5, deviations from the linear response are observed, indicating that the network hardens under shear.

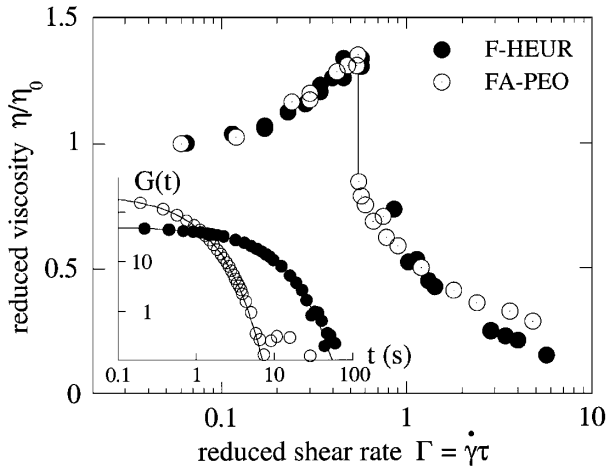

FIG. 1. Steady shear viscosity as a function of the applied shear rate in normalized units $\eta/\eta_0(\dot{\gamma}\tau)$ for two aqueous solutions of telechelic polymers (F-HEUR, closed symbols and FA-PEO, open symbols, both at $c = 4\%$). Inset: Stress relaxation functions $G(t)$ for the above two systems. The continuous lines are obtained using stretched exponentials with relaxation times $\tau = 0.6$ s (FA-PEO), $\tau = 6$ s (F-HEUR), and exponent ~0.8.

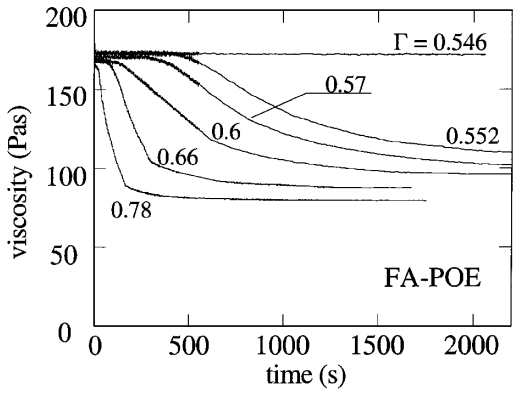

FIG. 2. Time dependence of the shear viscosity determined from start-up experiments close to the discontinuity evidenced for the FA-PEO solution in Fig. 1 ($c = 4\%$, $T = 25\,^{\circ}\mathrm{C}$).

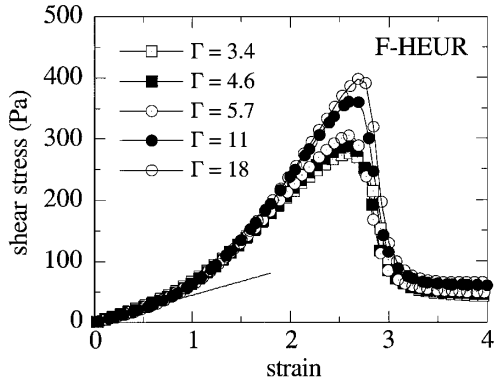

FIG. 3. Shear-stress responses obtained in start-up experiments on the F-HEUR solution ($c = 4\%$) for reduced shear rates $\Gamma = \dot{\gamma}\tau = 3-18$. The linear viscoelastic parameters for this sample are $G_0 = 53$ Pa, $\tau = 57$ s, and $\alpha = 0.81$ at $T = 20\,^{\circ}$C.

$\sigma(\gamma)$ culminates in a sharp maximum for deformations $\gamma \sim 2.5-2.8$ and drops towards the stationary limit. The representation of Fig. 3 was chosen to emphasize that the positions of the stress maxima are shear-rate independent. These last stress profiles are indeed similar to the load response characteristic of random networks at the rupture [11]. They are also reminiscent of the stress versus strain curves obtained in gelatin [12] or alginate [13] gels before breaking. In these cases, as in Fig. 3, the rupture is preceded by a nonlinear hardening regime and it occurs at a fixed strain, independent of the rate at which the load has been applied.

In order to demonstrate that telechelic polymer networks undergo a shear-induced fracture, we use a flow-visualization technique and determine the flow field under different shearing conditions. The flow-visualization device is a plate-plate transparent shearing cell mounted on an optical microscope. The configuration adopted was such that white light was sent through the 1.5 mm thick cell parallel to the velocity gradient direction. A constant rotation of the upper plate was applied stepwise so as to reproduce start-up experiments. Experiments at different shear rates were recorded by a CCD video camera and the trajectories of micron-size particles dispersed in the medium were digitized. For these experiments, a FA-PEO telechelic solution at $c = 3\%$ was specially prepared because of the adequacy between its relaxation time ($\tau =$ 2 s) and the experimental configuration.

The distances covered by particles located at different heights in the gap are shown in Fig. 4 as a function of the strain. This set of data represents the result of the digitalization of trajectories obtained during one start-up scenario at $\Gamma = 0.9$. At low deformations ($\gamma < 1.6$), these distances vary linearly, with a slope proportional to their respective velocities V_i. This initial slope allows us to determine the height of each particle within the gap. This height is comprised between some tens of microns (for particles that are the closest to the immobile plate) to 1.5 mm (for the upper plate, shown as a thick straight line).

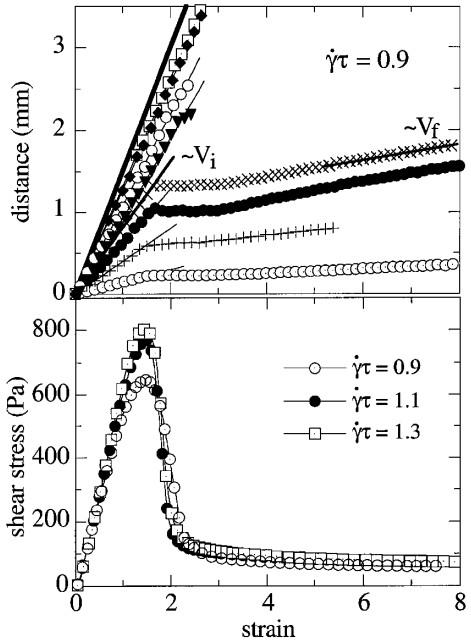

FIG. 4. Comparison between results of flow-visualization experiments and of rheology performed on a telechelic polymer network solution (FA-PEO, $c = 3\%$, room temperature). (Top panel): Distances covered by micron-sized particles dispersed in the fluid in a start-up experiment at $\Gamma = 0.9$. The plate-plate shearing cell is mounted on an optical microscope and the field of observation (2×2 mm^2) is located at 12 mm from the rotation axis (resolution ± 4 μm). The bold line gives the translation of a point on the upper rotating plate. The straight lines through the data points in the ranges $\gamma < 1.6$ and $\gamma \gg 1.6$ are proportional to V_i and V_f, respectively. (Bottom panel): Transient stress measurements obtained from start-up experiments at shear rates $\Gamma = 0.9$, 1.1, and 1.3 on the same solution.

For the particles belonging to the lower part of the cell, the distances covered during the start-up experiment of Fig. 4 exhibit a discontinuity of slope around $\gamma = 1.6$. Then, up to a deformation of 3, they stay immobile and accelerate again to reach a constant velocity V_f, which is much lower than the initial one. Both initial and final slopes (proportional to V_i and V_f, respectively) are indicated by straight lines in Fig. 4a. On the contrary, for the particles closest to the upper plate, no such discontinuity occurs ($V_i = V_f$). These dramatic changes in the velocity field can be compared to the stress data discussed previously. Transient stress measurements were performed in cone-and-plate geometry on the same FA-PEO solution. Stress versus strain results at shear rates $\Gamma = 0.9$, 1.1, and 1.3 are shown in the lower part of Fig. 4 and are in good agreement with the data of Fig. 3. The use of the same strain axis for the flow-visualization and rheology experiments in Fig. 4 allows us to ascribe unambiguously the abrupt drop of the stress to the onset of inhomogeneous flow.

The above flow-visualization experiments are summarized in Fig. 5, where the velocity fields V_i (a) and V_f (b) are displayed as functions of the height of the sheared fluid. At low deformation, the field is linear since we have

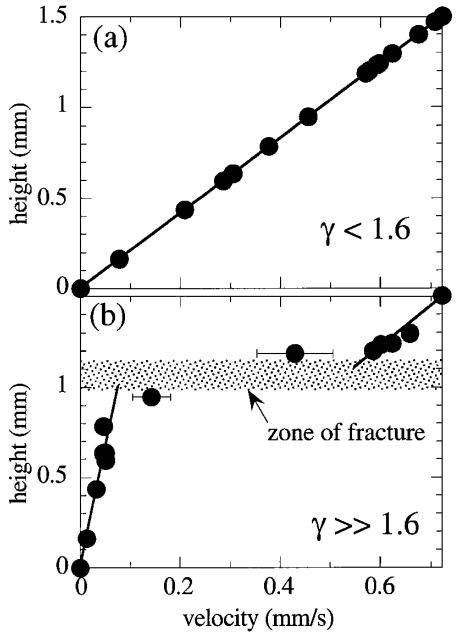

FIG. 5. Initial and stationary velocity fields deduced from the flow-visualization experiment shown in Fig. 4 for $\gamma < 1.6$ (a) and $\gamma \gg 1.6$ (b), respectively. At large deformations, the field exhibits a zone of fracture (shaded area) and the flow is inhomogeneous.

made the assumption of affinity to derive the heights of the particles. At large deformations, when all velocities are again stationary, the velocity field exhibits a zone of fracture and the flow is inhomogeneous. This zone of fracture is described as the part of the fluid submitted to a high shear rate ($\sim$10 times the applied rate) and where the stress probably arises from viscous dissipation. The elastic energy stored at the inception of shear is released around $\gamma = 1.6$ through the creation of "free" surfaces, free meaning here not connected by elastically active chains. Since the fracture zone in Fig. 5b is much broader than the average distance between cross-links ($\sim$300 Å), it is most likely that the fracture process is more complicated than a simple solid friction between two main macroscopic layers. These results deserve two additional comments. For the start-up scenario described in this Letter, the fracture zone is located at $2/3$ of the bottom plate. However, this fracture can happen everywhere in the gap. In most particles tracking experiments performed under the same experimental conditions, the fracture zone occurs generally at one of the interfaces, close to the moving or immobile plate. In these cases, the fracture appears as sliding, and the flow bears strong analogies with a plug flow. Even in this case, the phenomenology of the fracture remains identical to that described in Fig. 4. Such sliding effects were recently suspected in associative gels [4]. Second, it should be emphasized that due to the finite viscoelastic time of the network and contrary to ordinary gels investigated so far (as gelatin [12,14]), when the flow is stopped the fracture zone is healed. As expected, the healing of the fracture zone takes several τ's and is monitored by the equilibrium dynamics of connections and detachments of the end caps. After this delay, a new fracture can be produced and its location is independent of the previous one. Because of this healing effect, we call the phenomenon evidenced in Figs. 4 and 5 a fluid fracture. To our knowledge, this is one of the first evidences of a fracture reported in true viscoelastic liquids. It can be suggested in conclusion that the slow relaxations of the stress evidenced (Fig. 2) slightly above the discontinuity could result from a mechanism of nucleation and growth of cracks within the viscoelastic medium.

We thank D. Calvet, A. Collet, and M. Viguier from the Laboratoire "Organisation Moléculaire–Evolution et matériaux fluorés" at the Université de Montpellier II (France) for supplying us the polymers and for fruitful discussions.

[1] P. D. Olmsted, Europhys. Lett. **48**, 339 (1999).
[2] K. C. Tam, R. D. Jenkins, M. A. Winnik, and D. R. Bassett, Macromolecules **31**, 4149 (1998).
[3] Q. T. Pham, W. B. Russel, J. C. Thibeault, and W. Lau, Macromolecules **32**, 2996 (1999).
[4] T. Aubry, L. Blonce, and M. Moan, Appl. Rheol. **10**, 31 (2000).
[5] J.-F. Berret, Y. Séréro, B. Winkelman, D. Calvet, A. Collet, and M. Viguier, J. Rheol. **45**, 477 (2001).
[6] A. N. Semenov, J.-F. Joanny, and A. R. Khokhlov, Macromolecules **28**, 1066 (1995).
[7] M. A. Winnik and A. Yekta, Curr. Opin. Colloid Interface Sci. **2**, 424 (1997).
[8] D. Stauffer and A. Aharony, *Introduction to Percolation Theory* (Taylor & Francis, London, 1994).
[9] E. Alami, M. Rawiso, F. Isel, G. Beinert, W. Binana-Limbele, and J. François, ACS Adv. Chem. **248**, 343 (1996).
[10] N. Cathébras, A. Collet, M. Viguier, and J.-F. Berret, Macromolecules **31**, 1305 (1998).
[11] H. J. Herrmann and S. Roux, *Statistical Models for the Fracture of Disordered Media* (NHC, Amsterdam, 1990).
[12] R. D. Groot, A. Bot, and W. G. M. Agterof, J. Chem. Phys. **104**, 9202 (1996).
[13] C. Michon, G. Cuvelier, E. Aubrée, and B. Launay, Les Cahiers de Rhéologie **16**, 46 (1999).
[14] D. Bonn, H. Kellay, M. Prochnow, K. Ben-Djemiaa, and J. Meunier, Science **280**, 265 (1998).